doi:10.1016/S0022-2836(02)00879-3 available online at http://www.idealibrary.com on IDEAL® J. Mol. Biol. (2002) 323, 125–130

JMB

Structure of the Neutrophil-activating Protein from *Helicobacter pylori*

Giuseppe Zanotti[1,2]*, Elena Papinutto[1,2], William G. Dundon[2,3] Roberto Battistutta[1,2], Michela Seveso[3], Giuseppe Del Giudice[4] Rino Rappuoli[4] and Cesare Montecucco[2,3]

[1]*Dipartimento di Chimica Organica e Centro CNR Biopolimeri, Università di Padova, Via Marzolo 1 35131 Padova, Italy*

[2]*Venetian Institute of Molecular Medicine, VIMM Via Orus 2, 35129 Padova Italy*

[3]*Centro CNR Biomembrane e Dipartmento di Scienze Biomediche, Università di Padova, Via G. Colombo 3 35121 Padova, Italy*

[4]*CHIRON Research Laboratories, Via Fiorentina 1 53100 Siena, Italy*

**Corresponding author*

Helicobacter pylori is a major human pathogen associated with severe gastroduodenal diseases, including ulcers and cancers. An *H. pylori* protein that is highly immunogenic in humans and mice has been identified recently. This protein has been termed HP-NAP, due to its ability of activating neutrophils. In order to achieve a molecular understanding of its unique immunogenic and pro-inflammatory properties, we have determined its three-dimensional structure. Its quaternary structure is similar to that of the dodecameric bacterial ferritins (Dps-like family), but it has a different surface potential charge distribution. This is due to the presence of a large number of positively charged residues, which could well account for its unique ability in activating human leukocytes.

© 2002 Elsevier Science Ltd. All rights reserved

Keywords: neutrophil-activating protein; *Helicobacter pylori*; iron storage; ferritins; crystal structure

Introduction

Infection of humans with the Gram-negative bacterium *Helicobacter pylori* is associated with the development of severe gastroduodenal diseases, including chronic gastritis, peptic ulcers and stomach cancers.[1,2] A number of virulence factors produced by the bacterium have been identified. Among them, a relevant role is played by a 200 kDa protein called neutrophil-activating protein (HP-NAP). Its amino acid sequence presents significant similarities with *Escherichia coli* Dps, with *Listeria innocua* dodecameric ferritin (Flp) and with the two Dps-like proteins (Dlp-1 and Dlp-2) from *Bacillus anthracis*.[3–5] HP-NAP takes up iron *in vitro*,[6] increases the adhesion of neutrophils to endothelial cells,[7] induces migration and activation of human neutrophils and monocytes,[8,9] and is a potent stimulant of mast cells.[10] It binds to neutrophil-glycosphingolipids[11] and to mucin, a component of the stomach mucus layer.[12] HP-NAP is a major antigen in the human immune response to this bacterium[8,13] and as such is a component of an anti-*H. pylori* vaccine currently under clinical trial[13] (G.D.G. *et al.*, unpublished results). Given these unique properties of HP-NAP, it was of paramount importance to determine the atomic structure of this molecule, which is presented here.

Abbreviations used: HP-NAP, *Helicobacter pylori* neutrophil-activating protein; Dps, DNA-binding protein from starved cells; Flp, *Listeria innocua* ferritin; Dlp, Dps-like protein from *Bacillus anthracis*; MPD, 2-methyl-2,4-pentanediol.

E-mail address of the corresponding author: giuseppe.zanotti@unipd.it

Results and Discussion

The structure of the protein

HP-NAP, like the other members of this family, is a dodecamer, about 90 Å in diameter, with 32 symmetry (Figure 1). Each one of the 12 identical subunits has a folding very similar to that of Dps,

0022-2836/02/$ - see front matter © 2002 Elsevier Science Ltd. All rights reserved

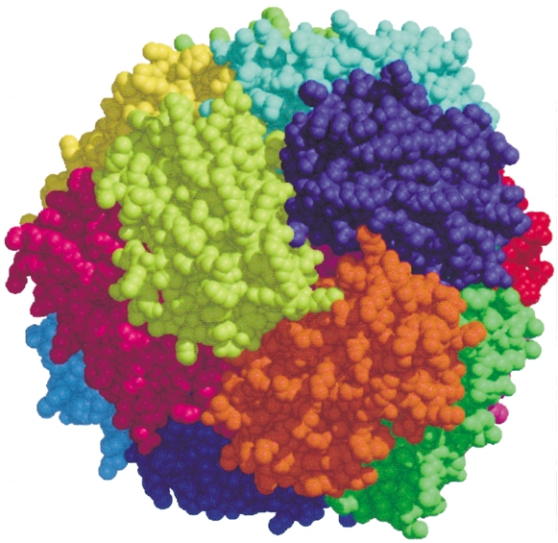

Figure 1. Van der Waals representation of the HP-NAP dodecamer. Each monomer is colored differently. One 3-fold axis is running approximately perpendicular to the plane of the paper in the center of the image, through one of the putative tunnels for the iron entrance.

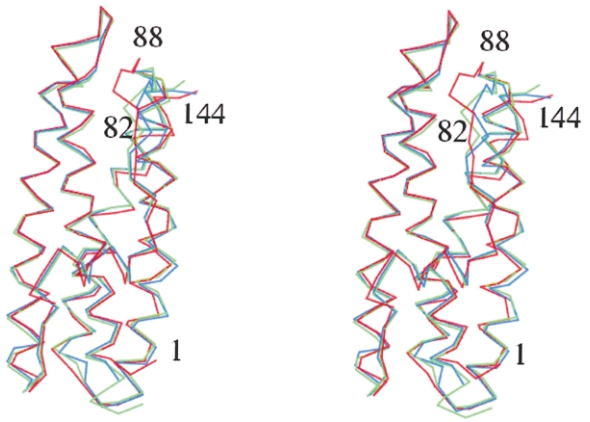

Figure 2. Stereo view of C^{α} trace of monomer of HP-NAP (red) superimposed on that of Dlp-1 (light blue) and Dlp-2 (green). The most significant difference is observed at the N terminus and in the region from 82 to 88, before helix C.

Flp, Dlp-1 and Dlp-2 from *B. anthracis*.[3–5] The superposition of the equivalent C^{α} atoms of the HP-NAP monomer to Dlp-1 and Dlp-2 yields a root-mean-square deviation of 0.9 Å (Figure 2). Significant differences between HP-NAP and Dlp-1 and Dlp-2 are observed in the long segment (Glu81-Ser88) that connects the N-terminal (helices A–B) and the C-terminal region (helices C–D).

The arrangement of the 12 monomers of HP-NAP results in a nearly spherical shell, with an internal cavity where iron is stored.[6] In the present crystal structure, the internal cavity is likely to be filled with unordered solvent molecules, and no iron was detected. The dodecamer possesses four 3-fold axes, each of them passing through the shell in two different 3-fold environments arranged as pores. One of the two 3-fold pores corresponds to the iron entry channel postulated for Flp.[4] This pore has a strongly hydrophilic and negatively charged environment. From the outside to the inside (Figure 3), one notices the presence of the side-chains of residues Glu114, Asp126 and Asp127 (and their symmetry mates). Of the three lysine residues around the pore surface, two of them (Lys107 and Lys115) are conserved in Flp, whilst the third (Lys119) is present only in HP-NAP. It replaces a negatively charged residue of Flp, Asp126. In the present structure, the tunnel is filled with a network of solvent molecules, designing a possible path for iron entry into the internal cavity. The second of the two 3-fold pores is smaller, it is partially hydrophilic (Thr31, Asp32, Asn35), and it is closed by the bulky side-chain of Phe34.

The internal surface of HP-NAP is strongly negatively charged: the α-helices 38–57 and 124–135 present nine negatively charged residues (five Glu and four Asp) per monomer, pointing their side-chains into the interior of the shell cavity. They form a negatively charged internal surface that is a common feature of ferritins and Dps-like proteins, and it is related to the original function of iron storage, retained by some members of this family.

Each subunit in the dodecamer makes strong interactions with the neighboring subunits: at least

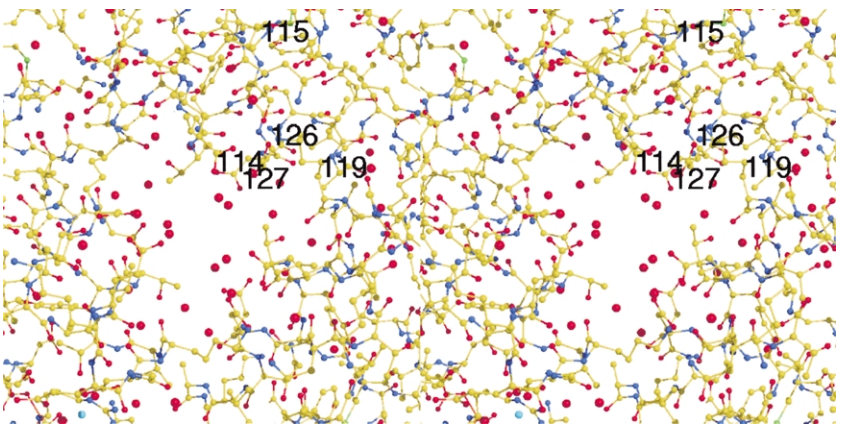

Figure 3. View of the residues that form the pore postulated to function as the entrance tunnel for iron ions. Charged residues present on the surface of the cavity and around the pore are labeled.

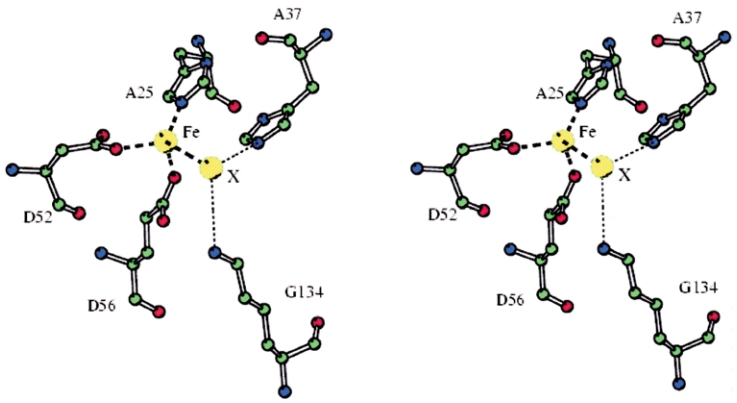

Figure 4. Stereo view of the iron site in HP-NAP. The iron atom is coordinated tetrahedrally by two oxygen atoms from subunit D and one nitrogen atom of a His from subunit A. The fourth coordination position is occupied by a solvent atom (X). The latter is at 3.6 Å from NE2 of His A37 and at 3.7 Å from NZ of Lys G134.

20 hydrogen-bond interactions per subunit can be identified in HP-NAP, accounting for its stability and resistance to denaturation.[6]

The metal-binding site

The 24-mer ferritins can bind cations other than Fe^{2+}, including Cd^{2+}, Zn^{2+}, Ca^{2+}, and Tb^{3+}.[14] In the case of HP-NAP, an X-ray fluorescence spectrum has indicated that iron is present in the crystal (not shown). A Fourier electron density map calculated with coefficients $|2F_{obs} - F_{calc}|$ presents one maximum per monomer with a value of 9σ and another one of 6σ. An iron atom refines in the position of the highest maximum with a reasonable thermal parameter ($B = 26$ Å^2) and its coordination is very similar to that of the Flp iron atom (Figure 4 and Table 1).[4] The cation environment has the features of tetrahedral coordination, where three corners are occupied by protein atoms (two oxygen atoms, one of Asp52 and the other of Glu56, from one monomer and a nitrogen atom of His25 from another monomer), whereas the fourth coordination position is occupied by a solvent molecule. However, its electron density (6σ) and its distance from the iron ion (3.05 Å), much longer than the mean distance of a coordination bond (Fe–O or Fe–N, 2–2.2 Å), do not account for a water oxygen atom. The fact that its electron density is compatible with an atom with more electrons than oxygen and its proximity with two other potentially positive side-chains (Lys134, 3.68 Å; His37, 3.59 Å) suggest the presence of a negative ion. Therefore, a chloride atom was refined in that position with a thermal *B* factor of 28 Å^2. HP-NAP displays *in vitro* ferroxidase activity[6] and the presence in iron coordination of carboxylate and histidine residues suggests that this site may function as a ferroxidase center, where the histidine residues are involved in the redox process.[15] All the ferroxidase centers so far described contain di-iron sites, with the two ions separated by a distance of about 3 Å. In the present model, it is unlikely that the isolated atom at a distance of 3.05 Å from the iron is the second iron atom, since it lacks the coordination typical of transition metals. We can hypothesize that a solvent molecule occupies exactly the position postulated for the second iron atom during the redox process. When the second iron is in place, a minimal rearrangement of the position of the side-chains of His37 and Lys134 can bring them to the correct distance for metal coordination.

Neutrophil activation

To date, HP-NAP is the only protein of the Dps family capable of activating human leukocytes. This property is so far unique, since the structurally similar Flp, Dlp-1 and Dlp-2 failed to activate human neutrophils (not shown). Therefore, we analyzed the surfaces of these proteins in an attempt to identify regions whose different properties could account for such a biological difference (Figure 5). The HP-NAP surface is characterized by a large presence of positively charged residues, a property not shared by the other members of the Dps family. The strong prevalence of positive charges of the electrostatic surface potential of HP-NAP confers a basic character on it. Positively charged residues of several proteins, including those of some chemokines, are believed to play a role in the activation of neutrophils.[16,17] Thus, it is

Table 1. Coordination distances of the metal-binding sites in HP-NAP

HP-NAP	*d* (Å)	Flp	*d* (Å)	Dlp-1	*d* (Å)	Dlp-2	*d* (Å)
Fe–X	3.05	Fe–O H_2O	3.1	Fe–O H_2O	1.95	Fe–O H_2O	2.06
Fe–NE2 His25	2.19	Fe–NE1 His31	2.3	Fe–NE1 His26	2.05	Fe–NE2 His29	2.10
Fe–OD1 Asp52	2.18	Fe–OD1 Asp58	1.8	Fe–OD2 Asp53	1.99	Fe–OD2 Asp56	2.00
Fe–OE2 Glu56	2.18	Fe–OE2 Glu62	2.3	Fe–OE1 Glu57	2.44	Fe–OE1 Glu60	1.97
X–NE2 His37	3.59	O H_2O–NE2 His43	2.7	–		–	

Distances for Flp are reported for comparison.

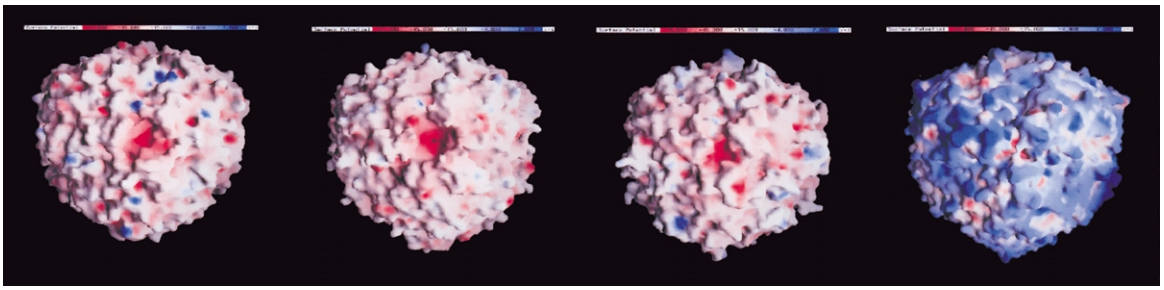

Figure 5. From right to left, electrostatic potential surface of HP-NAP, Flp from *L. innocua*, Dlp-2 and Dlp-1 from *B. anthracis*. The potential surface was calculated with the program GRASP.[23]

possible that the presence of a large number of basic residues on the HP-NAP dodecamer surface is responsible for its neutrophil-activating property. The availability of the HP-NAP structure will allow for a better understanding of the molecular basis of the strong immunogenicity of this important antigen and of its binding to glycosphyngolipids and to mucin. In addition, it will allow for the rational design of site-directed mutants to identify residues important in neutrophil activation.

Materials and Methods

Protein purification and crystallization

HP-NAP expressed in *Bacillus subtilis* was purified as described.[6] Two different crystal forms were obtained, both by using the vapor-diffusion technique either with hanging or sitting drops. In the first case, the crystals were grown using a solution containing 50 mM Tris–HCl (pH 8), 20% (w/v) PEG 8000 as precipitant. The crystal obtained belonged to the trigonal $R3$ space group, with $a = b = 88.8$ Å and $c = 423.6$ Å. For the second form, the precipitant solution used was 0.2 M ammonium acetate, 0.1 M citrate buffer (pH 5.6), 30% (v/v) 2-methyl-2,4-pentanediol (MPD). The crystals obtained were monoclinic, space group $P2_1$, with $a = 88.79$ Å, $b = 133.22$ Å and $c = 95.23$ Å. The latter is compatible with the presence of one dodecamer in the asymmetric unit, corresponding to a V_M of 2.78 Å^3/Da and a solvent content of about 55% (v/v).

Data collection and processing

Diffraction data were measured at the X-ray diffraction beam-line of the ELETTRA synchrotron in Trieste (Italy). One crystal of the approximate size of 0.15 mm × 0.15 mm × 0.1 mm allowed the measurement of an entire native data set. The monoclinic crystal was frozen at 100 K under a stream of cold nitrogen gas without the need of any cryoprotectant solution. During the measurements, the synchrotron ring was operated at 2.4 GeV and a wavelength of 1.3 Å was selected. Diffraction data were measured using an imaging-plate recorder (MAR Research, diameter 345 mm) positioned at a distance of 300 mm from the sample. 130 rotations of 1° and 68 oscillations of 0.5° were performed. Data were processed with the MOSFLM software[18] and reduced and merged with SCALA.[19] The statistics are reported in Table 2.

Structure determination and refinement

The structure of HP-NAP was solved using the molecular replacement method with the program AMoRe.[20] The initial search for the rotation function was performed at 5 Å resolution using the model of dodecameric Flp as template (PDB code 1QGH).[4] A set of equivalent solutions was found and all of them, subjected to a translation function, gave rise to the correct final solution that presented a crystallographic R factor of 0.52. Some cycles of rigid-body minimization reduced the R factor to 0.49. At this point, the model of HP-NAP with the correct amino acid sequence was introduced. After the first cycle of simulated annealing, the transformation matrices that relates the monomers in the dodecamer were obtained and, from that point, the refinement was carried out using only one monomer and imposing the strict non-crystallographic symmetry, as implemented in the CNS software package.[21] Model visualization and rebuilding was performed with QUANTA software (QUANTA, version 98.1111, Molecular Simulation, Inc., 1986-191). Some cycles of simulated annealing and energy minimization, followed by manual adjustments, reduced the crystallographic R factor to 0.25 (R_{free} = 0.26). At this point, two close maxima in the difference-Fourier map were interpreted as a possible iron site and a negative ion (see Results and Discussion). Water molecules were introduced in peaks of electron density close to hydrophilic residues and forming possible hydrogen bonds. Non-crystallographic symmetry was applied to solvent molecules and Fe atoms. An electron density accounting for an MPD molecule was visible in the difference-Fourier map in proximity to a

Table 2. Data collection and refinement statistics

A. *Data collection*	
Resolution (Å)	50–2.5 (2.66–2.52)
Independent reflections	71,729 (9698)
Multiplicity	2.9 (2.7)
Completeness (%)	96.7 (90.9)
$\langle I/\sigma(I)\rangle$	11.3 (5.9)
R_{merge}	0.045 (0.087)
B. *Refinement*	
Protein atoms	12 × 1196
Solvent molecules–Fe atoms	12 × 57
$R_{cryst.}$ (%)	21.5 (27.8)
R_{free} (%)	22.4 (28.6)
r.m.s. on bond distances (Å)	0.008
r.m.s. on bond angles (deg.)	1.7

The λ used for data collection was 1.36 Å. Numbers in parentheses refer to the last resolution shell. R_{free} was calculated with 10% of the data.

hydrophobic pocket, and it was introduced and refined. In the final model, it is close to residues 99 and 102, and one of its OH groups makes a hydrogen bond with OG1 of Thr135 and interacts with OH of Tyr99. All the residues in the sequence, from 1 to 144, were clearly visible and fitted in the electron density. The entire molecule was generated at the end of the refinement using the transformation matrices that relates the different subunits. An attempt to refine the entire molecular model using non-crystallographic restraints produced a lower R factor with a significant increase of the R_{free}. For this reason, we kept the 12 subunits virtually identical. The final model, whose statistics are reported in Table 2, consists of 12 identical groups of 1196 protein atoms, one iron atom and 56 solvent atoms each. The final crystallographic R factor is 0.215 ($R_{free} = 0.224$).

Quality of the final model

The quality of the model is quite good, and better than that expected at this relatively low resolution of 2.5 Å. The stereochemistry, as assessed by the program PROCHECK,[22] is quite satisfactory: 96% of the residues lie in the allowed and the other 4% in the generously allowed areas of the Ramachandran plot. The overall G-factor, 0.35, is better than the expected value for this resolution. This is largely due to the use of the strict non-crystallographic symmetry throughout all the refinement process, so that only 1253 atoms were treated independently. Consequently, the ratio of variables to observation was increased to 14, compared to the 1.2 value corresponding to the entire model treated independently.

Protein Data Bank accession code

Coordinates have been deposited at the RCSB Protein Data Bank with accession code 1JI4.

Acknowledgements

We thank the staff of the X-ray diffraction beamline of ELETTRA, Trieste, Italy, for technical assistance during data measurements. This work was supported by the Italian Ministero per l'Istruzione, l'Università e la Ricerca (MIUR) 40% Project on Inflammation, by the MURST-CNR Biotechnology Program L. 95/95, by the Armenise-Harvard Medical School Foundation and by the Italian National Research Council, Rome, Italy.

References

1. Goodwin, C. S. (1997). *Helicobacter pylori* gastritis, peptic ulcer, and gastric cancer: clinical and molecular aspects. *Clin. Infect. Dis.* **25**, 1017–1019.
2. Montecucco, C. & Rappuoli, R. (2001). Living dangerously: how *Helicobacter pylori* survives in the human stomach. *Nature Rev. Cell Biol.* **2**, 457–466.
3. Grant, R. A., Filman, D. J., Finkel, S. E., Kolter, R. & Hogle, J. M. (1998). The crystal structure of Dps, a ferritin homolog that binds and protects DNA. *Nature Struct. Biol.* **5**, 294–303.
4. Ilari, A., Stefanini, S., Chiancone, E. & Tsernoglou, D. (2000). The dodecameric ferritin from *Listeria innocua* contains a novel intersubunit iron-binding site. *Nature Struct. Biol.* **7**, 38–43.
5. Papinutto, E., Dundon, W., Pitulis, N., Battistutta, R., Montecucco, C. & Zanotti, G. (2002). Structure of two iron-binding proteins from *Bacillus anthracis*. *J. Biol. Chem.* **277**, 15093–15098.
6. Tonello, F., Dundon, W. G., Satin, B., Molinari, M., Tognon, G., Grandi, G. *et al.* (1999). The *Helicobacter pylori* neutrohil-activating protein is an iron-binding protein with dodecameric structure. *Mol. Microbiol.* **34**, 238–246.
7. Evans, D. J., Jr, Evans, D. G., Lampert, H. C. & Nakano, H. (1995). Identification of four new prokaryotic bacterioferritins, from *Helicobacter pylori*, *Anabaena variabilis*, *Bacillus subtilis* and *Treponema pallidum*, by analysis of gene sequences. *Gene*, **153**, 123–127.
8. Satin, B., Del Giudice, G., Della Bianca, V., Dusi, S., Laudanna, C., Tonello, F., Kelleher, D., Rappuoli, R., Montecucco, C. & Rossi, F. (2000). The neutrophil-activating protein (HP-NAP) of *Helicobacter pylori* is a protective antigen and a major virulence factor. *J. Exp. Med.* **191**, 1467–1476.
9. Montemurro, P., Barbuti, G., Dundon, W. G., Del Giudice, G., Rappuoli, R., Colucci, M. *et al.* (2001). *Helicobacter pylori* neutrophil-activating protein stimulates tissue factor and plasminogen activator inhibitor-2 production by human blood mononuclear cells. *J. Infect. Dis.* **183**, 1055–1062.
10. Montemurro, P., Nishioka, H., Dundon, W. G., de Bernard, M., Del Giudice, G., Rappuoli, R. & Montecucco, C. (2002). The neutrophil-activating protein (HP-NAP) of *Helicobacter pylori* is a potent stimulant of mast cells. *Eur. J. Immunol.* **32**, 671–676.
11. Teneberg, S., Miller-Podraza, H., Lampert, H. C., Evans, D. J., Jr, Evans, D. G., Danielsson, D. & Karlsson, K. A. (1997). Carbohydrate binding specificity of the neutrophil-activating protein of *Helicobacter pylori*. *J. Biol. Chem.* **272**, 19067–19071.
12. Namavar, F., Sparrius, M., Veerman, E. C., Appelmelk, B. J. & Vandenbroucke-Grauls, C. M. (1998). Neutrophil-activating protein mediates adhesion of *Helicobacter pylori* to sulfated carbohydrates on high-molecular-weight salivary mucin. *Infect. Immun.* **66**, 444–447.
13. Del Giudice, G., Covacci, A., Telford, J. L., Montecucco, C. & Rappuoli, R. (2001). The design of vaccines against *Helicobacter pylori* and their development. *Annu. Rev. Immunol.* **19**, 523–563.
14. Lawson, D. M., Artymiuk, P. J., Yewdall, S. J., Smith, J. M., Livingstone, J. C., Treffry, A. *et al.* (1991). Solving the structure of human H ferritin by genetically engineering intermolecular crystal contacts. *Nature*, **349**, 541–544.
15. Wade, V. J., Levi, S., Arosio, P., Treffry, A., Harrison, P. M. & Mann, S. (1991). Influence of site-directed modifications on the formation of iron cores in ferritin. *J. Mol. Biol.* **221**, 1443–1452.
16. Laurence, J. S., Blanpain, C., De Leener, A., Parmentier, M. & LiWang, P. J. (2001). Importance of basic residues and quaternary structure in the function of MIP-1 beta: CCR5 binding and cell surface sugar interactions. *Biochemistry*, **40**, 4990–4999.
17. Yang, Y., Mayo, K. H., Daly, T. J., Barry, J. K. & La Rosa, G. J. (1994). Subunit association and structural analysis of platelet basic-protein and related proteins

investigated by ^{1}H NMR spectroscopy and circular dichroism. *J. Biol. Chem.* **269**, 20110–20118.
18. Leslie, A. G. W. (1991). Molecular data processing. In *Crystallographic Computing V* (Moras, D., Podjarny, A. D. & Thierry, J. P., eds), pp. 50–61, Oxford University Press, Oxford.
19. Collaborative Computational Project Number 4 (1994). The CCP4 suite: programs for protein crystallography. *Acta Crystallog. sect. D*, **50**, 760–763.
20. Navaza, J. (1994). AMoRe: an automated package for molecular replacement. *Acta Crystallog. sect. A*, **50**, 157–163.
21. Brunger, A. T., Adams, P. D., Clore, G. M., DeLang, W. L., Gross, P., Grosse-Kunstleve, R. W. *et al.* (1998). Crystallography and NMR system: a new software suite for macromolecular structure determination. *Acta Crystallog. sect. D*, **54**, 905–921.
22. Laskowski, R. A., McArthur, M. W., Moss, D. S. & Thornton, J. (1993). PROCHECK: a program to check the stereochemical quality of protein structures. *J. Appl. Crystallog.* **26**, 283–291.
23. Nicholls, A., Sharp, K. A. & Honig, B. (1991). Protein folding and association: insights from the interfacial and thermodynamic properties of hydrocarbons. *Proteins: Struct. Funct. Genet.* **11**, 281–296.

Edited by R. Huber

(Received 18 April 2002; received in revised form 7 August 2002; accepted 13 August 2002)